Kalna, K. and Asenov, A. and Elgaid, K. and Thayne, I. (2000) Effect of impact ionization in scaled pHEMTs. In, *8th IEEE International Symposium on High Performance Electron Devices for Microwave and Optoelectronic Applications., 13-14 November 2000*, pages pp. 236-241, Glasgow, UK.

Effect of Impact Ionization in scaled pHEMTs

K. Kalna, A. Asenov, K. Elgaid and I. Thayne
Department of Electronics & Electrical Engineering
University of Glasgow, Glasgow, G12 8LT, Scotland, United Kingdom

Abstract:

The effect of impact ionization on pseudomorphic high electron mobility transistors is studied using Monte Carlo simulations when these devices are scaled into deep decanano dimensions. The scaling of devices with gate lengths of 120, 90, 70, 50 and 30 nm has been performed in both lateral and vertical directions. The impact ionization is treated as an additional scattering mechamism in the Monte Carlo module. The critical drain voltage, at which device characteristics begin to indicate breakdown, decreases as the gate voltage is lowered. Similarly, the breakdown drain voltage is also found to decrease during the scaling process.

I. Introduction

Pseudomorphic high electron mobility transistors (pHEMTs) with low indium content channels and channel lengths 0.25-0.15 μm are the workhorse of the MMIC industry today. However, there is potential for enhancing their performance by proper scaling to deep decanano dimensions [1]. We have recently reported an improvement in device transconductance when the gate length of pHEMTs is scaled from 120 nm to 90, 70, 50 and 30 nm [2], being limited ultimately by external resistances. In this paper, we revisit pHEMT scaling in the presence of the impact ionization effect, which is expected to be a crucial factor at large drain voltages causing a breakdown of the device [3]. This study is carried out in framework a large experimental programme in Glasgow aiming to establish Roadmap benchmarks for high-speed III-V devices. We will present a description of the impact ionization model and its verification, together with its implications for pHEMT scaling.

II. Monte Carlo module

We are using the finite element Monte Carlo device simulator (MC/H2F) [4] to investigate electron transport properties in the pHEMTs, fully scaled in both lateral and vertical direction. The MC/H2F uses quadrilateral finite elements to depict the complex geometry around the T-shape gate and recess as schematically drawn in Fig. 1. Our Monte Carlo module incorporates electron scattering with polar optical phonons, inter- and intra-valley optical phonons, non-polar optical and acoustic phonons and ionized and neutral impurity scattering. In addition, alloy scattering and strain effects [5] are considered in the InGaAs channel. All scattering rates consider a form factor (overlap integral) proposed by Matz [6] to extend validity of the analytic material band model up to electric fields of (>300-400 kV/cm) as depicted in Figs.2 and 3. Further details of our Monte Carlo module in the device simulator are given elsewhere [2,4].

III. Impact ionization model for analytic bands

Impact ionization has been incorporated into the MC/H2F device simulator as an additional scattering mechanism. An impact ionization event can only occur if the impacting electron gains enough energy to overcome the material bandgap, and hence any formula for impact ionization rate should be a function of this threshold energy, E_{th}. We have used a simple formula based on Keldysh's model [7] assuming that impact ionization is determined by the total phonon scattering rate

0-7803-6550-X/00/$10.00©2000 IEEE.

$\Gamma_{totalphonon}$ (E_{th}) at the threshold energy. Then the electron scattering rate due to the impact ionization can be expressed as [8]

$$\Gamma(E) = P\,\Gamma_{totalphonon}(E_{th})\left(\frac{E - E_{th}}{E_{th}}\right)^{A} \qquad (1)$$

where P and A are parameters which have to be fitted to experimental data as well as to scattering rate calculations using a full band model. The parameters P and A are first adjusted such that the impact ionization rate (1) as a function of electron energy is in good agreement with the rate obtained from full band MC simulation [9]. They are then fine tuned to experimental data by simulating the impact ionization coefficient in bulk as a function of the inverse applied electric field. Respective final angles are generated assuming that the final state of the impacting electron has no angle dependence on its initial state. A new electron is created in the Γ valley with a wavevector randomly chosen from a Gaussian distribution. A pair hole created in the impact ionization event is neglected – the Monte Carlo module is unipolar.

Fig. 4(a) compares the simulated impact ionization coefficient in GaAs with the experimental data of Refs. 10 and 11. Even in this very simple model assuming a parabolic dispersion, both the impact ionization rate and impact ionization coefficient exhibit very good agreement with the most recent experimental data of Ref. 11. However, Fig. 4(b) indicates that attempting to reproduce the impact ionization coefficient for $In_{0.53}Ga_{0.47}As$ is problematic due to the very narrow bandgap of this material. When compared to experimental data of Ref. 12, we are able to achieve a good fit at lower electric fields [between 4.5-5.2×10^{-6} cm/V in Fig. 4(b)] whereas the deviation dramatically increases at high electric fields. The scattering rates for $In_{0.53}Ga_{0.47}As$ obtained from Keldysh model and analytical bands do not agree with those rates obtained using an interaction matrix element of Fermi golden rule and a full band model [9]. The discrepancy arises due to different densities of states in each model at high electric fields. But we think that employing of Keldysh model for the impact ionization together with analytic bands is quite adequate approach and certainly much faster. Finally, due to the low indium content in the device channel a mistake introduced into the impact ionization rate of $In_{0.2}Ga_{0.8}As$ at high electric field is substantially reduced.

Simulated bulk drift velocities when impact ionization is included in the scattering mechanisms are depicted by open triangles in Fig. 2 and Fig. 3 for GaAs and $In_{0.53}Ga_{0.47}As$ respectively. The impact ionization sharply increases the drift velocity curve of bulk GaAs at fields greater than 400 kV/cm. This can be understood as follows. Electrons (mainly from the L or X valley) which have gained enough energy to cause the impact ionization fall to the Γ valley. Even though they have lost an amount of energy equal to the bandgap by undergoing this transition, their lower effective mass in the Γ valley allows them to possess higher velocities compared to those in the L and X valleys. Slightly different behaviour can be seen in the drift velocity curve of $In_{0.53}Ga_{0.47}As$. The drift velocity with impact ionization included is initially lower than that with impact ionization excluded and only afterwards sharply increases in the same manner as in GaAs. The narrower bandgap of $In_{0.53}Ga_{0.47}As$ allows impact ionization effects to start at field of only 200 kV/cm. At these fields the impacting electron ends up with a very small amount of energy and corresponding reduction in drift velocity, even allowing for the decrease in effective mass in the Γ valley. At larger electric fields of 300 kV/cm, the overall drift velocity of $In_{0.53}Ga_{0.47}As$ begins to behave like that of GaAs.

IV. Impact ionization breakdown in the scaled pHEMTs

The scaling investigation is based upon careful calibration of the MC simulations against I_D-V_D data from a 120-nm gate length pHEMT designed and fabricated at the University of Glasgow. The simulated I_D-V_D characteristics represent the behaviour of the intrinsic device. To compare this with experimental data, the effect of the contact resistances of the source and drain are included in the I_D-V_D curves at a post-processing stage. The final I_D-V_D characteristics (open symbols in Fig. 5) for V_G from -0.6 V to 0.4 V are in very good agreement with the experimental data (full symbols in Fig. 5). A rapid increase in the average velocity in the channel for the four fully scaled pHEMTs can be seen in Fig. 6. The inset of Fig. 6 shows how peaks of the channel velocity saturate with the further scaling of the devices to 50 and to 30 nm.

Fig. 7 indicates breakdown drain voltage, V_D^{br}, above which the drain current increases due to impact ionization events, to be 9.0, 7.5, 8.5, 8.0, 8.0, 7.5, 7.5, and 7.0 V, for V_G of 0.4, 0.2, 0.0, -0.2, -0.4, -0.6, -0.8, and -1.0 V, respectively. At these V_D^{br}, the drain current increases due to impact ionization events; the drain current increase from a relatively saturated I_D-V_D curve is deemed to signify the breakdown of the device. The I_D-V_D curves on Fig. 8, each plotted for a fixed V_G of -1.0 V, exhibit a substantial increase in drain voltage for all scaled devices. The sharp rise of the drain current above 4.0 V, even when the impact ionization is excluded, is primary related to the short channel effects which have increasing importance for shrinking devices. Fig. 8 demonstrates that the critical breakdown drain voltages decrease from 7.0 V to 6.5, 6.0, 5.0, and 4.5 V when the device is scaled from 120 to 90, 70, 50, and, finally, to 30 nm gate length, respectively. This can be understood quite straightforwardly as sufficiently high electric field allowing significant impact ionization can be reached at lower drain voltages as the distance between the drain and source is reduced. Therefore, a reduction in the operating voltage window of pHEMTs is expected as the device scales more down. This calls for the importance of choice in supply voltage.

The breakdown drain voltages in our simulations appear to be large as compared to some experiments [3] which indicate a lower breakdown voltage in HEMTs. We have not found any experimental indication of the device breakdown up to the drain voltage of 6.0 V at the gate voltage of 0.0 V in our real 120-nm gate length pHEMT. Further, breakdown drain voltages of the GaN MESFET device calculated from MC device simulations [13] were reported to be much larger then the voltages from drift-diffusion simulations and are in the same range as ours.

The reason for discrepancy with experimental data [3] in our simulations is the exclusion of holes created by impact ionization. Hole generation and transport reduces the field between the source and substrate, driving a positive feedback loop responsible for earlier device breakdown. Other limitations of this study are asociated with the incorporation of impact ionization effects within an analytical band structure model. It is well known that any impact ionization rate is principally dependent on the density of states. To obtain the density of states accurately at high electric fields, full band MC device simulators are required which calculate the band material structure using, e.g., the non-local pseudopotential method.

V. Conclusion

We have carried out a Monte Carlo study of the pHEMTs breakdown with the low indium content when these devices are scaled into the deep decanano dimensions. The impact ionization responsible for a device breakdown has been incorporated into the Monte Carlo module of the device simulator as an additional scattering mechanism. The formula originally proposed by Keldysh has been employed after being calibrated to experimental data in bulk Monte Carlo simulations.

The whole simulation study is based on the careful calibration of the Monte Carlo device simulator against a real 120-nm gate length device. We have found an indication of the device breakdown at quite large drain voltages. The breakdown voltage decreases when the gate voltage is decreasing from 0.4 V to -1.0 V. When the devices are scaled down proportionally from the gate length of 120 nm to 90, 70, 50 and, finally, to 30 nm then the breakdown drain voltage is also lowered as expected.

References:

[1] U. K. Mishra, A. S. Brown, L. M. Jelloian, L. H. Hackett, and M. J. Delaney, "High-performance submicrometer AlInAs-GaInAs HEMT's", *IEEE Electron Device Lett.* (1988) **9,** 41-42.
[2] K. Kalna, A. Asenov, K. Elgaid and I. Thayne, "Scaling of pHEMTs to decanano dimensions", to appear in *VLSI design* (2000).
[3] G. Meneghesso, T. Grave, M. Manfredi, M. Pavesi, C. Canali, and E. Zanoni, Analysis of hot carrier transport in AlGaAs/InGaAs pseudomorphic HEMT's by means of electroluminescence}, *IEEE Trans. Electron Devices* (2000) **47,** 2-10.
[4] S. Babiker, A. Asenov, J. R. Barker, and. P. Beaumont, "Finite element Monte Carlo simulation of recess gate compound FETs", *Solid St. Electron.* (1996) **39**, 629-635.
[5] Ch. Köpf, H. Kosina and S. Selberherr, "Physical models for strained and relaxed GaInAs alloys: band structure and low-field transport", *Solid St. Electron.* (1997) **41**, 1139-1152.
[6] D. Matz, "Effects of nonparabolicity on non-ohmic transport in InSb and InAs", *Phys. Rev.* (1968) **168**, 843-844.
[7] L. V. Keldysh, "Behavior of non-metallic crystals in strong electric field", *Sov. Phys. JETP* (1958) **6(33)**, 763-770.
[8] M. Stobbe, R. Redmer, and W. Schattke, "Impact ionization rate in GaAs", *Phys. Rev.* B (1994) **49**, 4494-4500.
[9] N. Sano and A. Yoshii, "Impact-ionization model consistent with the band structure of semiconductors", *J. Appl. Phys.* (1995) **77**, 2020-2025.
[10] S. N. Shabde and C. Yeh, "Ionization rates in (Al_xGa_{1-x})As," *J. Appl. Phys.* (1970) **41**, 4743-4744.
[11] H. D. Law and C. A. Lee, "Interband scattering effects on secondary ionization coefficients in GaAs," *Solid-State Electron.*, (1978) **21**, 331-340.
[12] T. P. Pearsall, "Impact ionization rates for electron and holes in $In_{0.53}Ga_{0.47}As$," *Appl. Phys. Lett.* (1980) **36**, 218-220.
[13] M. Farahmand and K. F. Brennan, "Full band Monte Carlo simulation of Zincblende GaN MESFET's including realistic impact ionization rates", *IEEE Trans. Electron Devices* (1999) **46**, 1319-1325.

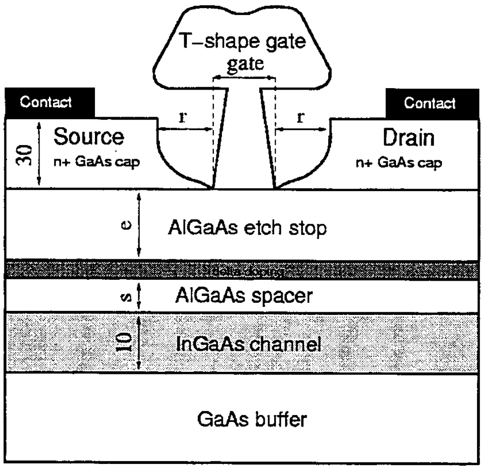

Figure 1: Cross-section of pHEMTs as represented in the simulator.

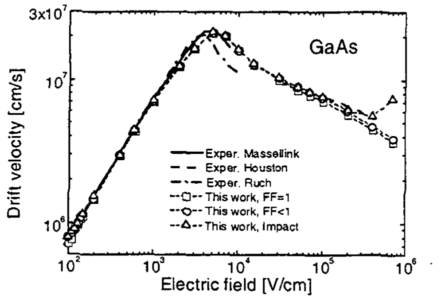

Figure 2: Drift velocity versus applied electric field in GaAs. The simulated results considering the form factor (FF) equal to 1, by Ref. 6, and including impact ionization are compared with various experimental data.

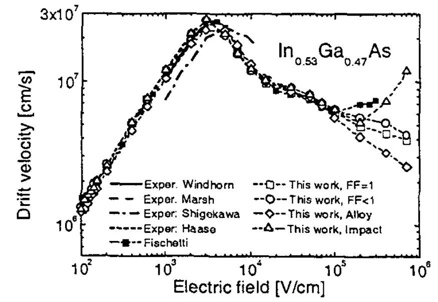

Figure 3: Drift velocity versus applied electric field in $In_{0.53}Ga_{0.47}GaAs$. The simulated results considering the form factor (FF) equal to 1, by Ref. 6, and including alloy scattering or impact ionization are compared with various experimental and simulated data.

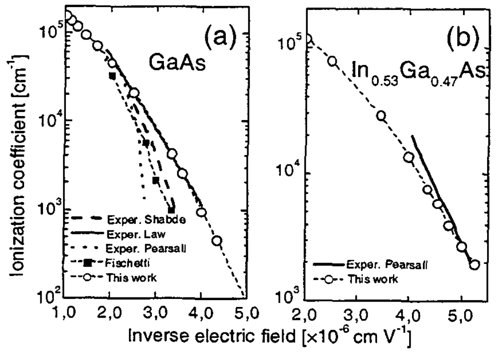

Figure 4: Impact ionization coefficients versus inverse applied electric field obtained from simulations for GaAs (a) and for $In_{0.53}Ga_{0.47}GaAs$ (b) are compared with experiments and full band simulations.

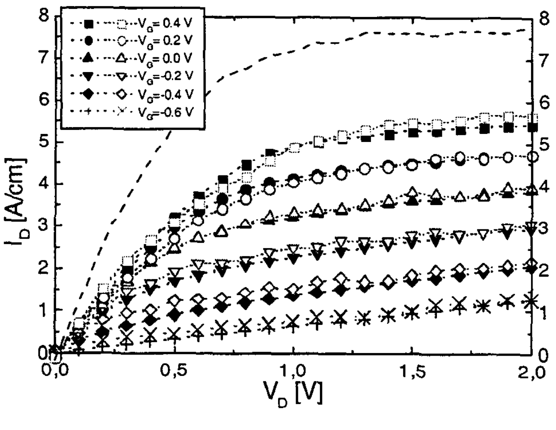

Figure 5: I-V characteristic of the calibrated pHEMT with a gate length of 120 nm. Full symbols are experimental data for several fixed gate voltages V_G. Open symbols represent MC simulations when external resistances of the drain and source are included. The I-V characteristic for an intrinsic device (dashed line) is shown for comparison, for a gate voltage of 0.4 V.

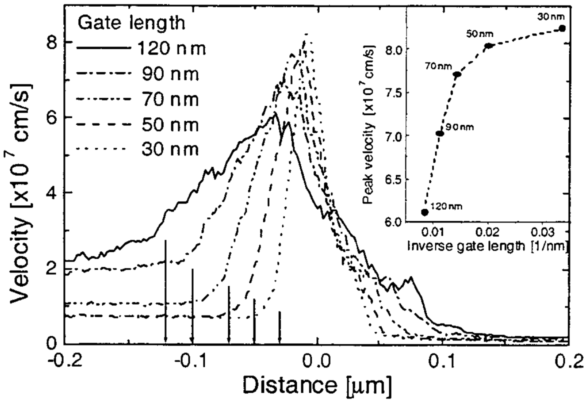

Figure 6: Average velocities along the InGaAs channel for a set of the scaled pHEMTs when drain and gate voltages are 1.5 V and 0.0 V, respectively. The arrows indicate a beginning of the channel when its end is set to zero. The inset shows a saturation of peak average velocity during the scaling process.

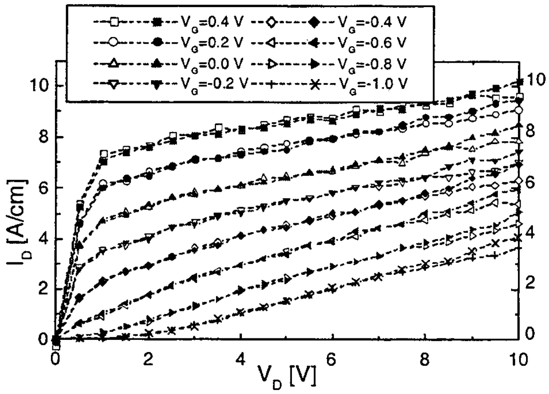

Figure 7: I-V characteristic for a 120-nm gate length intrinsic device for several fixed V_G when impact ionization is excluded (open symbols) and included (full symbols).

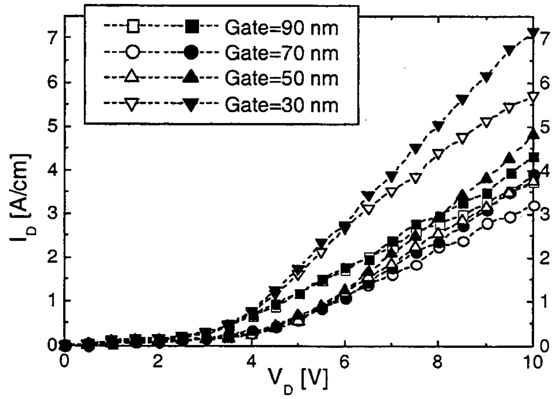

Figure 8: I-V characteristic of an intrinsic device for gate lengths of 90, 70, 50 and 30 nm, respectively, for fixed V_G of -1.0 V. Open symbols are simulations without the impact ionization and full symbols with the impact ionization.